Inorg. Chem. **2002**, *41*, 4194–4205

Heterobimetallic Bismuth–Transition Metal Salicylate Complexes as Molecular Precursors for Ferroelectric Materials. Synthesis and Structure of $Bi_2M_2(sal)_4(Hsal)_4(OR)_4$ (M = Nb, Ta; R = CH_2CH_3, $CH(CH_3)_2$), $Bi_2Ti_3(sal)_8(Hsal)_2$, and $Bi_2Ti_4(O^iPr)(sal)_{10}(Hsal)$ (sal = $O_2CC_6H_4$-2-O; Hsal = $O_2CC_6H_4$-2-OH)

John H. Thurston and Kenton H. Whitmire*

Department of Chemistry, Rice University, 6100 Main Street, Houston, Texas 77005

Received February 18, 2002

The reactions between triphenylbismuth, salicylic acid, and the metal alkoxides $M(OCH_2CH_3)_5$ (M = Nb, Ta) or $Ti\{OCH(CH_3)_2\}_4$ have been investigated under different reaction conditions and in different stoichiometries. Six novel heterobimetallic bismuth alkoxy–carboxylate complexes have been synthesized in good yield as crystalline solids. These include $Bi_2M_2(sal)_4(Hsal)_4(OR)_4$ (M = Nb, Ta; R = CH_2CH_3, $CH(CH_3)_2$), $Bi_2Ti_3(sal)_8(Hsal)_2$, and $Bi_2Ti_4(O^iPr)(sal)_{10}(Hsal)$ (sal = $O_2CC_6H_4$-2-O; Hsal = $O_2CC_6H_4$-2-OH). The complexes have been characterized spectroscopically and by single-crystal X-ray diffraction. Compounds of the group V transition metals contain metal ratios appropriate for precursors of ferroelectric materials. The molecules exhibit excellent solubility in common organic solvents and good stability against unwanted hydrolysis. The nature of the thermal decomposition of the complexes has been explored by thermogravimetric analysis and powder X-ray diffraction. We have shown that the complexes are converted to the corresponding oxide by heating in an oxygen atmosphere at 500 °C. The mass loss of the complexes, as indicated by thermogravimetric analysis, and the resulting unit cell parameters of the oxides are consistent with the formation of the desired heterobimetallic oxide. The complexes decomposed to form the bismuth-rich phases $Bi_4Ti_3O_{12}$ and $Bi_5Nb_3O_{15}$ as well as the expected oxides $BiMO_4$ (M = Nb, Ta) and $Bi_2Ti_4O_{11}$.

Introduction

Heterometallic alkoxide or carboxylate complexes are attractive molecular precursors for bimetallic or multimetallic oxide materials. These complexes may be amenable for use in sol−gel synthesis,[1] metal-organic chemical vapor deposition (MOCVD),[2] or metal-organic decomposition type syntheses of oxides.[3] Using discrete, well-defined molecular precursors may allow control of the metal composition of these complexes so that they could be used as single-source precursors for advanced ceramics. A single source precursor may lead to a higher quality of product because of the intimate mixing of the different metals achieved at the molecular level.[4] Single source precursors are also attractive because they present a direct route to advanced materials and because they may require lower temperatures or shorter calcination periods to be converted to the correct oxide phase than conventional solid-state methods. Lower preparation temperatures allow the materials to be deposited on a broader range of substrates.

A number of bismuth oxide containing materials have desirable properties, including high T_c superconductivity,[5,6] nonlinear optical properties,[7] and high oxide ion mobility in the solid state.[8] Of particular significance is a series of

* To whom correspondence should be addressed. E-mail: whitmir@ruf.rice.edu.

(1) Park, Y.; Nagai, M.; Miyayama, M. *J. Mater. Sci.* **2001**, *36*, 1261−1269.
(2) Hironaka, K.; Isobe, C.; Moon, B. *Jpn. J. Appl. Phys.* **2001**, *40*, 680−686.
(3) Hou, Y.; Xu, X.; Wang, H. *Appl. Phys. Lett.* **2001**, *78*, 1733−1735.
(4) Annika, I.; Pohl, M.; Westin, L. G.; Kritikos, M. *Chem.—Eur. J.* **2001**, *7*, 3438−3445.
(5) Maeda, H.; Tanaka, Y.; Fukutomi, M.; Asano, T. *Jpn. J. Appl. Phys.* **1988**, *27*, L209.
(6) Hodge, P.; James, S.; Norman, N.; Orpen, A. *J. Chem. Soc., Dalton Trans.* **1998**, 4049−4054.
(7) Parola, S.; Papiernik, R.; Hubert-Pfalzgraf, L. G.; Jagner, S.; Hakansson, M. *J. Chem. Soc., Dalton Trans.* **1998**, 737−739.
(8) Pell, J. W.; Davis, W. C.; Loye, H. C. z. *Inorg. Chem.* **1996**, *35*, 5754.

10.1021/ic0255454 CCC: $22.00
Published on Web 07/18/2002

layered oxide materials known as the Aurivillius phases. All of the Aurivillius phases show ferroelectric behavior and are therefore potential candidates for ferroelectric random access memories (FRAM).[9] The composition of the Aurivillius phases can be expressed by the general formula $(Bi_2O_2)^{2+}$-$(A_{n-1}B_nO_{3n+1})^{2-}$ where A and B can be any metal ion with the appropriate charge-to-radius ratio.[10] Most commonly, A is Bi, Pb, Sr, Ca, or K, and B is Ti, Zr, Nb, Ta, Mo, W, Fe, and Co. Of all the potential combinations that have been created from the general formula, those containing titanium, niobium, or tantalum have shown the greatest promise for the development of significant ferroelectric materials. Examples of these compounds are $SrBi_2Nb_2O_9$, $BaBi_2Ta_2O_9$, and $Bi_4Ti_3O_{12}$. These compounds exhibit retention of a high dielectric constant, low leakage current, and good ferroelectric switching characteristics.[7,9,11]

The importance of bismuth-containing layered oxide materials and the lack of well-characterized heterometallic alkoxide and carboxylate complexes have prompted us to investigate the synthesis and characterization of complexes of bismuth with group IV or group V transition metals. There is relatively little structural information available for heterobimetallic alkoxide or carboxylate complexes of bismuth. Known compounds are limited to several alkali or alkaline-earth metal species such as $KBi(O^tBu)_4$,[12] $Na_2Bi_4O_2(OC_6F_5)_{10}$,[13] $Bi_4Ba_4(\mu_6\text{-}O)_2(\mu_3\text{-}OEt)_8(\mu\text{-}OEt)_4(\eta^2\text{-}thd)_4$,[7] and $Na_4Bi_2(\mu_6\text{-}O)(OC_6F_5)_8(THF)_4$.[14] A few bismuth−transition metal alkoxide complexes such as $[BiCl_3OV(OC_2H_4OMe)_3]_2$,[8] $BiTi_2(\mu_3\text{-}O)(\mu\text{-}O^iPr)_4(O^iPr)_5$,[15] and $Cp_2MoBi(\mu_2\text{-}OEt)_2(OEt)_2Cl$ ($Cp = C_5H_5$)[16] have been reported. Bismuth−molybdenum allyl carbonyl complexes such as $[(\mu_3\text{-}CHC(CH_3)CH_2)Mo(CO)_2(\mu_2\text{-}OEt)_3Bi(OEt)]_2$ have been characterized.[17] Also, two substituted polyoxometalates of general composition $[NBu_4]_3[M_4Mo(\mu_5\text{-}O)_2(\mu_2\text{-}OMe)_4(\mu_2\text{-}O)_8(NO)(O)_4]_2Bi$ (M = Mo, W) are known.[18] Of the compounds reported, $[BiCl_3OV(OC_2H_4OMe)_3]_2$, $Cp_2MoBi(\mu_2\text{-}OEt)_2(OEt)_2Cl$, and many of the allyl−molybdenum complexes contain halide ions that would likely act as a contaminant of the final oxide material. The polyoxometalates do not contain the correct stoichiometry of metals to make them useful precursors for the formation of the ferroelectric Aurivillius phases. This leaves only $BiTi_2(\mu_3\text{-}O)(\mu\text{-}O^iPr)_4(O^iPr)_5$, $Bi_4Ba_4(\mu_6\text{-}O)_2(\mu_3\text{-}OEt)_8(\mu\text{-}OEt)_4(\eta^2\text{-}thd)_4$, $Mo_2Bi_2(CO)_4(\mu^2\text{-}OCH_2CH_3)_8(\eta^3\text{-}CH_2C(CH_3)CH_2)_2$, and possibly $[MoBi(CO)_2(\mu^2\text{-}OCH_2CH_2OCH_3)_3(\eta^3\text{-}CH_2C(CH_3)CH_2)(THF)][BF_4]$ as well-characterized potential precursors for advanced ferroelectric materials.

We wish to report here the synthesis and characterization of six new heterobimetallic complexes of bismuth, $Bi_2M_2(sal)_4(Hsal)_4(OR)_4$ (**1a**, M = Nb, R = $CH(CH_3)_2$; **2a**, M = Ta, R = $CH(CH_3)_2$; **1b**, M = Nb, R = CH_2CH_3; **2b**, M = Nb, R = CH_2CH_3), $Bi_2Ti_3(sal)_8(Hsal)_2$ (**3**), and $Bi_2Ti_4(O^iPr)(sal)_{10}(Hsal)$ (**4**) (sal = $O_2CC_6H_4$-2-O) (Hsal = $O_2CC_6H_4$-2-OH). All of the complexes demonstrate good solubility in most common organic solvents and greatly improved stability against hydrolysis compared to the monometallic metal alkoxides, making these compounds attractive potential precursors for advanced materials. Powder X-ray diffraction studies of the complexes reveal that under the conditions used, the complexes decomposed yielding known bimetallic oxides. Calcination of **1b** and **2b** produced the expected $BiMO_4$ (M = Nb, Ta) as the major product in both cases, with small amounts of $Bi_5Nb_3O_{15}$ and Bi_2O_3 being detected in the two samples, respectively. Interestingly, **3** and **4** decomposed to produce the ferroelectric oxide phase $Bi_4Ti_3O_{12}$ as the major crystalline phase while the expected $Bi_2Ti_4O_{11}$ was produced in comparatively small amounts.

Experimental Section

General Procedures. All manipulations were performed under an atmosphere of dry nitrogen or argon using standard Schlenk and glovebox techniques. Solvents were dried over an appropriate reagent under argon and were distilled immediately prior to use. $Ti(O^iPr)_4$, $Nb(OEt)_5$, $Ta(OEt)_5$, $BiPh_3$, $PbPh_4$ (Strem), and salicylic acid (Aldrich Chemical Co.) were used as received. Galbraith Laboratories performed elemental analyses of all of the complexes. Infrared spectra were recorded on a Nicolet Nexus 670 FT-IR instrument using attenuated total reflectance (ATR) or on a Nicolet 205 FT-IR as Nujol mulls. NMR data were collected at 298 K on a Bruker 200, 400, or 500 MHz instrument and were referenced to the protio impurity in the deuterated solvent (^1H) or to tetramethylsilane (^{13}C) as an internal standard. Chemical shifts are reported in parts per million (ppm), while coupling constants are given in hertz (Hz). Coupling constants were not resolved for the aromatic protons of **1a**, **1b**, **2a**, or **2b**. The following abbreviations are employed in the descriptions of the spectra: s singlet, d doublet, t triplet, q quartet, h heptet, br broad, Ar aryl. The ipso carbon of the salicylate ligand was generally not resolved, even with extended collection times. This can be attributed to the relaxation time of this quaternary carbon. Powder X-ray diffraction studies were performed on a Siemens D5000 Diffraktometer, using Cu Kα radiation ($\lambda = 1.54$ Å). Data were collected on 2θ from 10° to 65° at 0.1° increments with 10 s exposures per frame. Mass spectra of **3** were taken on a Finnigan MAT-95 instrument, using high-temperature EI (HTEI) techniques. A 100 eV cone voltage was employed in the experiments. The sample was volatilized by heating the probe from ambient temperature to 800 °C over the course of 8 min. Data were collected in the range $m/z = 500-2500$. Repeated attempts to study samples **1a**, **2a**, **1b**, **2b**, and **4** using DEI, MALDI, FAB^+, ESI, and HTEI techniques did not produce meaningful data. The solution phase molar masses of complexes **1b** and **3** were determined in THF, using literature procedures.[19] Tetraphenyl lead was used as the reference standard in the solution phase molar mass

(9) Zhou, Q. F.; Chan, H. L. W.; Choy, C. L. *J. Non-Cryst. Solids* **1999**, *254*, 106−111.
(10) Sugimoto, W.; Shirata, M.; Sugahara, Y.; Kuroda, K. *J. Am. Chem. Soc.* **1999**, *121*, 11601−11602.
(11) Du, X.; Chen, I. *Mater. Res. Soc. Symp. Proc.* **1998**, *493*, 261−266.
(12) Veith, M.; Yu, E.; Huch, V. *Chem.−Eur. J.* **1995**, *1*, 26.
(13) Whitmire, K. H.; Hoppe, S.; Sydora, O.; Jolas, J. L.; Jones, C. M. *Inorg. Chem.* **2000**, *39*, 85−97.
(14) Jolas, J.; Hoppe, S.; Whitmire, K. *Inorg. Chem.* **1997**, *36*, 3335−3340.
(15) Parola, S.; Papiernik, R.; Hubert-Pfalzgraf, L. G.; Jagner, S.; Hakansson, M. *J. Chem. Soc., Dalton Trans.* **1997**, 4631.
(16) Hunger, M.; Limberg, C.; Kircher, P. *Angew. Chem., Int. Ed.*. **1999**, *38*, 1105.
(17) Hunger, M.; Limberg, C.; Kircher, P. *Organometallics* **2000**, *19*, 1044.
(18) Villanneau, R.; Proust, A.; Robert, F.; Gouzerh, P. *J. Chem. Soc., Dalton Trans.* **1999**, 421.
(19) Francis, J. A.; McMahon, C. N.; Bott, S. G.; Barron, A. R. *Organometallics* **1999**, *18*, 4399−4416.

experiments. For the TGA/DTA analyses, approximately 5 mg of the complex to be studied was placed in a platinum pan in the furnace of a Seiko TGA/DTA 200 instrument. The sample was heated to 600 °C at a rate of 10 °C/min. The mass loss of each sample was monitored and compared to that expected for the formation of the heterobimetallic oxide. Phase changes in the product heterobimetallic oxide were monitored by DTA.

Synthesis. Reactions of $BiPh_3$ with Salicylic Acid. Bismuth salicylate ($Bi\{Hsal\}_3$) can be prepared through the stoichiometric reaction of triphenyl bismuth (0.440 g, 1.0 mmol) with salicylic acid (0.441 g, 3.0 mmol) in refluxing toluene. The complex formed in this method is very poorly soluble and precipitates from solution, leading us to assume that it is oligomeric. The product of this reaction analyzes for the expected $Bi(salH)_3$ composition: % obsd (% calcd for $BiC_{21}H_{15}O_9$) C, 40.51 (40.66); H, 2.76 (2.44). IR: ν(COO) cm^{-1} 1320, 1575, 1599, 1621, 1650; ν(OH) cm^{-1} 3231. We have found that the use of excess salicylic acid (>7 equiv) does not lead to precipitation. Optimal conditions for the syntheses were found to be ca. 20 equiv of salicylic acid per bismuth. In this case, the resulting bismuth complex is soluble in a wide range of solvents. Meaningful elemental analyses of that complex have not been obtained because of contamination by excess salicylic acid. The complex is most soluble when it is used directly after it has been prepared. This methodology was employed for the syntheses of the heterobimetallic complexes discussed in this paper.

$Bi_2M_2(sal)_4(Hsal)_4(OR)_4$ (1a, M = Nb, R = $CH(CH_3)_2$; 2a, M = Ta, $CH(CH_3)_2$). The procedure for the synthesis of these compounds is similar, so only a general method will be reported here. Triphenylbismuth (0.440 g, 1.0 mmol) and salicylic acid (3.03 g, 22 mmol) were combined in 20 mL of toluene. The suspension was refluxed for 1 h, and then, the solvent was removed under reduced pressure. The yellow solid residue was dissolved in 10 mL of a 1 M solution of water in 2-propanol to give a clear colorless solution. Dropwise addition of $Nb(OEt)_5$ (0.5 mL, 2.0 mmol) resulted in a clear yellow solution, which was allowed to stand undisturbed for two weeks. During this time, yellow crystals deposited in the flask. The crystals were collected by filtration, washed with 2-propanol (3 × 10 mL) and pentane (5 mL), and then dried in vacuo. Single crystals suitable for X-ray diffraction were obtained directly from the reaction mixture. Yield (**1a**): 0.58 g (60%). Anal. % obsd (% calcd for $Bi_2Nb_2C_{68}H_{64}O_{28}$): C, 42.32 (42.26); H, 3.39 (3.34). ^{1}H NMR ($CDCl_3$): 1.1 (d, C*H*$_3$, 6H, J_{H-H} = 4.2 Hz), 3.9 (sp, C*H*, 1H, J_{H-H} = 4.2 Hz), 6.5 (br s, Ar*H*), 7.0 (br s, Ar*H*), 7.3 (br s, Ar*H*), 7.8 (br s, Ar*H*), 11.0 (br s, O*H*). ^{13}C NMR {^{1}H}(C_6D_6): −30.6 (*C*H$_3$), 63.3 (*C*H), 111.4 (Ar*C*), 118.6 (Ar*C*), 119.7 (Ar*C*), 129.7 (Ar*C*), 131.7 (Ar*C*), 136.9 (*C*OH), 162.8-(*C*O$_2$). IR: ν(COO) 1349, 1571, 1591, 1616. TGA: % loss (% calcd for formation of $BiNbO_4$) 62% (62%). Yield (**2a**): 0.51 g (48%). Anal. % obsd (% calcd for $Bi_2Ta_2C_{68}H_{64}O_{28}$): C, 38.60 (38.72); H, 3.27 (3.06). ^{1}H NMR ($CDCl_3$): 1.1 (d, C*H*$_3$, 6H, J_{H-H} = 6.9 Hz), 3.9 (sp, C*H*, 1H, J_{H-H} = 6.9 Hz), 6.9−7.9 (br mult). ^{13}C{^{1}H} NMR (C_6D_6): −30.4 (*C*H$_3$), 63.1 (*C*H), 118.3 (Ar*C*), 119.0 (Ar*C*), 129.5 (Ar*C*), 131.7 (Ar*C*), 137.0 (*C*OH), 162.8 (*C*O$_2$). IR: ν(COO) 1352, 1568,1593, 1622. TGA: % loss (% calcd for formation of $BiTaO_4$) 55% (57%).

$Bi_2M_2(sal)_4(Hsal)_4(OR)_4$ (1b, M = Nb, R = CH_2CH_3; 2b, M = Ta, CH_2CH_3). The procedure for the synthesis of these two complexes is similar, so only a general method will be described here. Triphenylbismuth (0.440 g, 1.0 mmol) and salicylic acid (0.554 g, 4.0 mmol) were refluxed in 20 mL of toluene under argon for 1 h. After, the reaction period, the yellow suspension was cooled to room temperature, and tantalum ethoxide (0.26 mL, 1.0 mmol) was added slowly with stirring. The clear solution was stirred for 15 h at room temperature. The product was isolated by removal of the solvent under reduced pressure, followed by extraction of the residue with dichloromethane (20 mL) and filtration. The filtrate was layered with hexane and stored at −20 °C for 2 days, which resulted in the growth of white needles. These crystals were collected by filtration and stored under nitrogen. Yield (**1b**): 0.51 g (54%). Anal. % obsd (% calcd for $Bi_2Nb_2C_{64}H_{56}O_{28}$): C, 37.44 (37.44); H, 3.00 (2.75). ^{1}H NMR (C_6D_6): 0.9 (t, C*H*$_3$, 3H, J_{H-H} = 4.1 Hz), 3.3 (q, C*H*$_2$, 2H, J_{H-H} = 4.1 Hz), 6.4 (s, Ar*H*), 6.6−7.0 (mult, Ar*H*), 7.7 (s, Ar*H*). ^{13}C NMR {^{1}H}(C_6D_6): 30.6 (*C*H$_3$), 63.3 (*C*H$_2$), 118.6 (Ar*C*), 119.7 (Ar*C*), 128.9 (Ar*C*), 131.7 (Ar*C*), 136.9 (*C*OH), 162.8 (CO_2). IR ν(COO): 1352s 1572s, 1591s, 1618s. TGA: % loss (% calcd for formation of $BiNbO_4$) 59% (61%). Yield (**2b**): 0.67 g (71%). Anal. % obsd (% calcd for $Bi_2Ta_2C_{64}H_{56}O_{28}$): C, 40.18 (40.95); H, 3.28 (3.01). ^{1}H NMR (C_6D_6): 0.9 (t, C*H*$_3$), 3.3 (q, C*H*$_2$), 6.3 (q), 6.5−7.0 (mult), 7.8 (s). ^{13}C{^{1}H} NMR (C_6D_6): 18.6 (*C*H$_3$), 21.8 (*C*H$_2$), 118.5 (Ar*C*), 119.7 (Ar*C*), 129.7 (Ar*C*), 131.6 (Ar*C*), 137.0 (*C*OH), 163.1 (CO_2). IR: ν (COO) 1352s, 1593s, 1622s, 1660s. TGA: % loss (% calcd for formation of $BiTaO_4$) 56% (56%).

$Bi_2Ti_4(O^iPr)(sal)_{10}(Hsal)\cdot 3HO^iPr\cdot H_2O$ (3). Triphenylbismuth (0.440 g, 1.0 mmol) and salicylic acid (3.03 g, 22 mmol) were combined in 20 mL of toluene. The suspension was refluxed for 1 h, and then, the solvent was removed under reduced pressure. The yellow solid residue was redissolved in 10 mL of a 1 M solution of water in 2-propanol to give a clear colorless solution. Dropwise addition of 0.6 mL of $Ti(O^iPr)_4$ (2.0 mmol) resulted in a clear orange-red solution, which was allowed to stand undisturbed for two weeks. During this time, red crystals deposited in the flask. The crystals were collected by filtration, washed with 2-propanol (3 × 10 mL) and pentane (5 mL), and dried in vacuo. Single crystals suitable for X-ray diffraction were obtained directly from the reaction mixture. Yield (**3**): 0.41 g (0.2 mmol, 75%). Anal. % obsd (% calcd for $Bi_2Ti_4C_{80}H_{52}O_{34}\cdot 3C_3H_8O\cdot H_2O$): C, 45.51 (45.54); H, 2.97 (3.29). ^{1}H NMR ($CDCl_3$): 1.2 (d, C*H*3, 6H, 6.1 Hz), 4.7 (septet, C*H*, 1H, 6.1 Hz), 6.2−8.3 (mult, Ar*H*, 1.7 Hz), 9.1 (br s, O*H*). ^{13}C{^{1}H} NMR ($CDCl_3$): 25.8 (*C*H$_3$), 64.9 (*C*H), 125.7 (Ar*C*), 128.6 (Ar*C*), 129.4 (Ar*C*), 131.3 (Ar*C*), 138.3 (*C*OH), 163.4 (*C*O$_2$). HTEIMS: 2169 (M^+, 30%), 2113 (**A**, M^+− O^iPr, 35%), 2052 (**B**, M^+− sal, 44%), 1991 (**A** − sal, 57%), 1929 (**B** − sal, 80%), 1865 (**A** − 2sal, 100%), 1801 (**B** − 2sal, 95%), 1734 (**A** − 3sal, 70%), 1668 (**B** − 3sal, 53%), 1600 (**A** − 4sal, 26%), 1531 (**B** − 4sal, 23%), 1460 (**A** − 5sal, 23%). IR: ν(COO) 1391, 1579, 1600, 1604. TGA: % loss (% calcd for formation of $Bi_2Ti_4O_{11}$) 61% (60%).

$Bi_2Ti_3(sal)_8(Hsal)_2\cdot 3CH_2Cl_2$ (4). Triphenylbismuth (0.440 g, 1.0 mmol) and salicylic acid (0.551 g, 4 mmol) were combined in 20 mL of toluene. The suspension was refluxed for 1 h. During this time, a yellow precipitate developed. Dropwise addition of 0.3 mL of $Ti(O^iPr)_4$ (1.0 mmol) resulted in an immediate color change to deep orange and dissolution of all of the solid. The resulting solution was stirred at room temperature for 15 h, and then, the solvent was evaporated to dryness under reduced pressure. The orange residue was extracted with 20 mL of CH_2Cl_2 and filtered through Celite. The clear orange filtrate was layered with hexane, and solvent diffusion was allowed to occur. After 3 days, large orange crystals had deposited along with a yellow powder. Samples for X-ray analysis were taken from this solution. The title complex was isolated by decanting the mother liquor from the crystalline solid, followed by washing with 2-propanol until the filtrate no longer became yellow (~3 × 15 mL). The residue was washed with pentane (1 × 15 mL) and dried well under vacuum to yield an orange microcrystalline solid. Yield (**4**): 0.41 g (75%, based on bismuth). Anal. % obsd (% calcd for $Bi_2Ti_3C_{70}H_{42}O_{30}\cdot 3CH_2$-

Table 1. Crystallographic Data for New Compounds

	$C_{68}H_{64}Bi_2Nb_2O_{28}$	$C_{68}H_{64}Bi_2O_{28}Ta_2$	$C_{80}H_{52}Bi_2O_{35}Ti_4$	$C_{70}H_{42}Bi_2O_{30}Ti_3$
fw	1932.97	2109.05	2182.78	2179.47
space group	$P\bar{1}$ (No. 2)	$P\bar{1}$ (No. 2)	$P2_1/n$ (No. 14)	$P\bar{1}$ (No. 2)
Z	1	1	4	2
cryst syst	triclinic	triclinic	monoclinic	triclinic
a (Å)	11.231(2)	11.361(2)	15.143(3)	13.320(3)
b (Å)	12.997(3)	13.090(3)	33.020(7)	13.654(3)
c (Å)	13.615(3)	13.675(3)	19.147(4)	23.377(5)
α (deg)	65.83(3)	66.06(3)	90	82.98(3)
β (deg)	72.49(3)	71.89(3)	108.75(3)	83.68(3)
γ (deg°)	85.07(3)	84.27(3)	90	66.35(3)
V, Å^3	1727.5(6)	1765.9(6)	9066(3)	3856.5(13)
D(calcd), g·cm^{-1}	1.858	1.983	1.599	1.877
temp (°C)	−50	25	−50	25
λ, Mo Kα (Å)	0.71073	0.71073	0.71073	0.71073
μ (cm^{-1})	54.87	81.40	42.86	51.39
R1[a]	0.0356	0.0367	0.0598	0.0311
wR2[b]	0.0911	0.1071	0.1376	0.0835

[a] Conventional R on F_{hkl}: $\sum|F_o| - |F_c|/\sum|F_o|$. [b] Weighted R on $|F_{hkl}|^2$: $\{\sum w(F_o^2 - F_c^2)^2/\sum[w(F_o^2)^2]\}^{1/2}$.

Cl_2): C, 39.87 (40.22); H, 1.34 (2.22). ^{1}H NMR ($CDCl_3$): 5.8−8.2 (mult, Ar*H*, J_{H-H} = 1.7 Hz). $^{13}C\{^1H\}$ NMR ($CDCl_3$): 116.6 (Ar*C*), 117.7 (Ar*C*), 121.8 (Ar*C*), 122.2 (Ar*C*), 132.5 (Ar*C*), 136.5 (*C*OH), 165.0 (*C*O_2). TGA: % obsd (% calcd for formation of $Bi_2Ti_3O_9$) 63.5% (63.1%). IR: ν(COO) cm^{-1} 1362, 1388, 1529, 1573, 1599, 1622.

Crystal Structure Determination. Crystals of all compounds were manipulated under argon using standard inert atmosphere techniques. Data collection and refinement parameters are given in Table 1. Complexes **1a**, **3**, and **4** were studied on a Bruker Smart 1000 diffractometer equipped with a CCD area detector (θ_{max} = ~24°). The data were corrected for Lorentz and polarization effects and for absorption (SADABS).[20] Complex **2a** was mounted and studied on a Bruker-Nonius κ diffractometer (θ_{max} = 33.4°). Several reflection intensities were monitored throughout data collection, and no decay of the crystals was detected. All data were corrected for Lorentz and polarization effects and absorption (empirical). Heavy atoms were located using direct methods with the SHELXTL software package.[21] All other non-hydrogen atoms were located by successive Fourier maps and were refined using the full-matrix least-squares method on F^2. Hydrogen atoms were included in calculated positions and refined using a riding model. All non-hydrogen atoms in complexes **1a**, **2a**, and **4** were refined anisotropically. Complex **3** suffered from a systematic disorder of ca. 20 2-propanol molecules per unit cell. Solvent effects were removed from the data using the program SQUEEZE in the PLATON software package.[22] The structure was refined similarly to the other molecules using SHELXTL. Only the metal atoms in the structure were refined anisotropically because of the limited data set. The weakness of the data is attributable to the massive solvent disorder and is discussed in more detail in the Results section.

Results

Triphenylbismuth reacts with salicylic acid (1:3) in refluxing toluene to produce a stable yellow complex that precipitates from solution. When this stoichiometry is employed, the product is soluble only in coordinating solvents such as THF and methanol. The elemental analysis of the solid produced in this reaction supports the formulation as $[Bi(O_2CC_6H_4OH)_3]_n$. The solubility of the bismuth salicylate product changes when using excess salicylic acid during the synthesis. When a 20:1 ratio of acid to $BiPh_3$ is used, the product displays good solubility not only in coordinating solvents such as THF and alcohols but also in hot toluene.

Table 2. Bond Lengths [Å] and Angles [deg] for $C_{68}H_{64}Bi_2Nb_2O_{28}$ (**1a**)

Bi(1)−O(43)	2.195(4)	Nb(2)−O(51)	1.834(4)
Bi(1)−O(13)	2.242(4)	Nb(2)−O(61)	1.851(4)
Bi(1)−O(33)	2.322(4)	Nb(2)−O(11)	1.935(4)
Bi(1)−O(32)	2.532(4)	Nb(2)−O(21)	1.959(4)
Bi(1)−O(42)	2.621(5)	Nb(2)−O(22)	2.069(4)
Bi(1)−O(23)#1[a]	2.628(4)	Nb(2)−O(12)	2.182(4)
O(43)−Bi(1)−O(13)	81.91(16)	O(42)−Bi(1)−O(23)#1	74.01(14)
O(43)−Bi(1)−O(33)	77.14(16)	O(51)−Nb(2)−O(61)	99.5(2)
O(13)−Bi(1)−O(33)	81.76(15)	O(51)−Nb(2)−O(11)	97.48(19)
O(43)−Bi(1)−O(32)	72.33(17)	O(61)−Nb(2)−O(11)	98.60(19)
O(13)−Bi(1)−O(32)	131.64(14)	O(51)−Nb(2)−O(21)	101.9(2)
O(33)−Bi(1)−O(32)	53.32(14)	O(61)−Nb(2)−O(21)	87.33(18)
O(43)−Bi(1)−O(42)	52.93(15)	O(11)−Nb(2)−O(21)	158.49(17)
O(13)−Bi(1)−O(42)	78.68(15)	O(51)−Nb(2)−O(22)	89.79(18)
O(33)−Bi(1)−O(42)	128.18(15)	O(61)−Nb(2)−O(22)	166.74(18)
O(32)−Bi(1)−O(42)	113.31(15)	O(11)−Nb(2)−O(22)	89.51(17)
O(43)−Bi(1)−O(23)#1	124.74(16)	O(21)−Nb(2)−O(22)	81.44(16)
O(13)−Bi(1)−O(23)#1	72.90(15)	O(51)−Nb(2)−O(12)	170.94(17)
O(33)−Bi(1)−O(23)#1	142.25(14)	O(61)−Nb(2)−O(12)	89.45(18)
O(32)−Bi(1)−O(23)#1	154.56(15)	O(11)−Nb(2)−O(12)	79.47(16)
O(21)−Nb(2)−O(12)	79.94(16)	O(22)−Nb(2)−O(12)	81.69(16)

[a] Symmetry transformations used to generate equivalent atoms: #1 $-x+2, -y+2, -z+1$.

The bismuth salicylate complex produced from the reaction of 1 equiv of triphenylbismuth with 20 equiv of salicylic acid reacts with the metal alkoxides $Ti\{OCH(CH_3)_2\}_4$ and $M(OCH_2CH_3)_5$ (M = Nb, Ta) to produce heterobimetallic complexes in good yield under mild conditions. 2-Propanol was found to be a good solvent for the niobium and tantalum reactions, and in this solvent, rapid exchange of the ethoxide ligands for 2-propoxide occurs as anticipated. The complexes precipitate from the solvent and can be isolated as stable, crystalline solids. The aggregation and growth of early transition metal complexes under similar conditions have been documented.[23,24] We have also demonstrated that similar reactions are possible using stoichiometric amounts of carboxylic acid in the reaction mixture in the case of complexes **1b**, **2b**, and **4**. Complexes **1a**, **2a**, **3**, and **4** have been characterized by single-crystal X-ray diffraction. Selected crystallographic data and bond distances for the data are presented in Tables 1−5. Diagrams of the complexes, along with the adopted numbering schemes of the metals, are presented in Figures 1−6. Complexes **1a** and **2a** are isolated from the reaction solutions as yellow or colorless cubic isomorphous crystals, respectively. The transition metal atoms in both molecules exist in distorted octahedral environments, retaining two terminal alkoxide ligands and

(20) Sheldrick, G. *SADABS* 5.1; University of Göttingen: Göttingen, Germany, 1997.
(21) Sheldrick, G. *SHELXTL* 6.1; University of Göttingen: Göttingen, Germany, 2001.
(22) Spek, A. L. *Platon, A Multipurpose Crystallographic Tool*; Utrecht University: Utrecht, The Netherlands, 2001.
(23) Kickelbick, G.; Schubert, U. *J. Chem. Soc., Dalton Trans.* **1999**, 1301−1305.
(24) Kickelbick, G.; Schubert, U. **1998**, *198*, 159−161.

Table 3. Bond Lengths [Å] and Angles [deg] for $C_{68}H_{64}Bi_2O_{28}Ta_2$ (**2a**)

Bi(1)−O(13)	2.204(6)	Ta(1)−O(41)	1.839(6)
Bi(1)−O(23)	2.253(5)	Ta(1)−O(61)	1.855(6)
Bi(1)−O(53)	2.346(5)	Ta(1)−O(21)	1.940(6)
Bi(1)−O(52)	2.548(5)	Ta(1)−O(31)	1.964(6)
Bi(1)−O(12)	2.626(7)	Ta(1)−O(32)	2.061(5)
Bi(1)−O(33)#1[a]	2.645(5)	Ta(1)−O(22)	2.162(5)
O(13)−Bi(1)−O(23)	81.9(2)	O(12)−Bi(1)−O(33)#1	73.56(18)
O(13)−Bi(1)−O(53)	78.1(2)	O(41)−Ta(1)−O(61)	99.6(3)
O(23)−Bi(1)−O(53)	81.0(2)	O(41)−Ta(1)−O(21)	97.5(3)
O(13)−Bi(1)−O(52)	73.0(2)	O(61)−Ta(1)−O(21)	98.2(3)
O(23)−Bi(1)−O(52)	131.01(19)	O(41)−Ta(1)−O(31)	101.4(3)
O(53)−Bi(1)−O(52)	53.37(18)	O(61)−Ta(1)−O(31)	88.5(3)
O(13)−Bi(1)−O(12)	52.8(2)	O(21)−Ta(1)−O(31)	158.6(2)
O(23)−Bi(1)−O(12)	78.4(2)	O(41)−Ta(1)−O(32)	89.8(2)
O(53)−Bi(1)−O(12)	128.6(2)	O(61)−Ta(1)−O(32)	167.5(2)
O(52)−Bi(1)−O(12)	114.5(2)	O(21)−Ta(1)−O(32)	88.7(2)
O(13)−Bi(1)−O(33)#1	124.4(2)	O(31)−Ta(1)−O(32)	81.4(2)
O(23)−Bi(1)−O(33)#1	73.3(2)	O(41)−Ta(1)−O(22)	171.3(2)
O(53)−Bi(1)−O(33)#1	141.61(19)	O(61)−Ta(1)−O(22)	89.0(2)
O(52)−Bi(1)−O(33)#1	154.6(2)	O(21)−Ta(1)−O(22)	79.4(2)
O(31)−Ta(1)−O(22)	80.4(2)	O(32)−Ta(1)−O(22)	82.0(2)

[a] Symmetry transformations used to generate equivalent atoms: #1 $-x+1, -y+1, -z+1$.

two chelating salicylate ions. The niobium−oxygen bond lengths range from 1.834(4) to 2.182(4) Å in **1a**. The tantalum−oxygen bond distances range from 1.839(6) to 2.162(5) Å in **2a**. The shortest bonds, which are associated with the alkoxide ligands in both cases, are those that are approximately trans to the carboxylate group of a salicylate ligand. These carboxylate−metal bonds are the longest M−O distances in the molecule.

The bismuth atoms are also six-coordinate, but the geometry at the metal center is severely distorted from an octahedral or trigonal prismatic environment (Figure 7). The bismuth atoms possess two terminal salicylate ligands that chelate the metal through the carboxylate functionality. A third salicylate ion bridges between the bismuth atom and the transition metal. The coordination sphere of the metal is completed by dative interactions to a fourth carboxylate ligand.

In both **1a** and **2a**, the aromatic ring of each of the bridging ligands is bent toward one of the bismuth atoms suggesting a weak π-interaction (Figures 1 and 7). The distance between the ring centroid and the bismuth atom is 3.393 Å in the case of **1a** and is 3.410 Å in the case of **2a**. The bismuth−oxygen bond lengths in the complexes vary over a large range. In **1a**, the bond distances range from 2.195(4) to 2.628(4) Å. In **2a**, the bond lengths range from 2.204(6) to 2.645(5) Å. There appears to be a rough correlation in each case between the bond lengths so that a long metal−oxygen bond is located approximately trans to a short metal−oxygen bond. In addition, the chelating salicylate ligands that are bound only to the bismuth atom each contain one long and one short metal oxygen bond. The shortest metal oxygen bond is roughly trans to the coordinated aromatic ring.

Compound **3** is isolated as deep red prisms. The molecule was found to be asymmetric, containing six metal atoms in a variety of coordination environments. As in **1a** and **2a**, the transition metals in **3** are six-coordinate and exist in distorted octahedral environments. The Ti−O bond lengths

Table 4. Bond Lengths [Å] and Angles [deg] for $C_{80}H_{52}Bi_2O_{35}Ti_4$ (**3**)

Bi(1)−O(123)	2.195(11)	Ti(2)−O(121)	1.815(10)
Bi(1)−O(92)	2.223(10)	Ti(2)−O(83)	1.849(11)
Bi(1)−O(71)	2.275(10)	Ti(2)−O(31)	1.881(11)
Bi(1)−O(63)	2.438(11)	Ti(2)−O(122)	2.037(11)
Bi(1)−O(91)	2.494(10)	Ti(2)−O(32)	2.053(10)
Ti(1)−O(111)	1.730(9)	Ti(2)−O(82)	2.069(10)
Ti(1)−O(101)	1.878(11)	Ti(3)−O(11)	1.822(10)
Ti(1)−O(23)	1.881(10)	Ti(3)−O(43)	1.852(10)
Ti(1)−O(33)	2.031(11)	Ti(3)−O(61)	1.853(10)
Ti(1)−O(102)	2.058(10)	Ti(3)−O(42)	2.007(9)
Ti(1)−O(22)	2.141(10)	Ti(3)−O(12)	2.022(10)
Bi(2)−O(21)	2.174(10)	Ti(3)−O(62)	2.032(10)
Bi(2)−O(13)	2.245(9)	Ti(4)−O(52)	1.802(9)
Bi(2)−O(81)	2.338(10)	Ti(4)−O(73)	1.827(9)
Bi(2)−O(59)	2.382(10)	Ti(4)−O(41)	1.988(10)
Bi(2)−O(12)	2.576(10)	Ti(4)−O(103)	2.009(11)
Bi(2)−O(22)	2.699(9)	Ti(4)−O(51)	2.031(9)
Bi(2)−C(17)	2.808(16)	Ti(4)−O(72)	2.048(9)
O(123)−Bi(1)−O(92)	74.5(4)	O(123)−Bi(1)−O(63)	88.1(4)
O(123)−Bi(1)−O(71)	76.4(4)	O(92)−Bi(1)−O(63)	80.1(3)
O(92)−Bi(1)−O(71)	80.4(3)	O(71)−Bi(1)−O(63)	157.8(3)
O(123)−Bi(1)−O(91)	124.7(4)	O(102)−Ti(1)−O(22)	84.2(4)
O(92)−Bi(1)−O(91)	54.3(3)	O(21)−Bi(2)−O(13)	76.1(4)
O(71)−Bi(1)−O(91)	75.9(4)	O(21)−Bi(2)−O(81)	84.6(4)
O(63)−Bi(1)−O(91)	101.2(4)	O(13)−Bi(2)−O(81)	79.4(3)
O(123)−Bi(1)−C(97)	100.5(5)	O(21)−Bi(2)−O(59)	91.8(3)
O(92)−Bi(1)−C(97)	28.3(4)	O(13)−Bi(2)−O(59)	70.1(3)
O(71)−Bi(1)−C(97)	75.6(4)	O(81)−Bi(2)−O(59)	149.2(3)
O(63)−Bi(1)−C(97)	92.0(4)	O(21)−Bi(2)−O(12)	129.3(3)
O(91)−Bi(1)−C(97)	26.1(4)	O(13)−Bi(2)−O(12)	54.1(3)
O(111)−Ti(1)−O(101)	97.9(5)	O(81)−Bi(2)−O(12)	78.4(3)
O(111)−Ti(1)−O(23)	99.7(5)	O(59)−Bi(2)−O(12)	80.5(3)
O(101)−Ti(1)−O(23)	93.5(5)	O(21)−Bi(2)−O(22)	52.4(3)
O(111)−Ti(1)−O(33)	92.4(5)	O(13)−Bi(2)−O(22)	116.5(3)
O(101)−Ti(1)−O(33)	164.8(5)	O(81)−Bi(2)−O(22)	122.5(3)
O(23)−Ti(1)−O(33)	95.9(5)	O(59)−Bi(2)−O(22)	76.6(3)
O(111)−Ti(1)−O(102)	93.9(5)	O(12)−Bi(2)−O(22)	157.1(3)
O(101)−Ti(1)−O(102)	85.0(4)	O(21)−Bi(2)−C(17)	102.6(4)
O(23)−Ti(1)−O(102)	166.4(4)	O(13)−Bi(2)−C(17)	26.6(4)
O(33)−Ti(1)−O(102)	83.1(4)	O(81)−Bi(2)−C(17)	80.9(4)
O(111)−Ti(1)−O(22)	174.3(5)	O(59)−Bi(2)−C(17)	70.1(4)
O(101)−Ti(1)−O(22)	87.3(4)	O(12)−Bi(2)−C(17)	27.9(3)
O(23)−Ti(1)−O(22)	82.2(4)	O(22)−Bi(2)−C(17)	137.6(4)
O(33)−Ti(1)−O(22)	82.1(4)	O(121)−Ti(2)−O(83)	94.9(6)
O(121)−Ti(2)−O(31)	98.4(5)	O(42)−Ti(3)−O(12)	79.6(4)
O(83)−Ti(2)−O(31)	98.6(5)	O(11)−Ti(3)−O(62)	165.3(5)
O(121)−Ti(2)−O(122)	84.7(4)	O(43)−Ti(3)−O(62)	99.8(4)
O(83)−Ti(2)−O(122)	94.1(5)	O(61)−Ti(3)−O(62)	84.2(4)
O(31)−Ti(2)−O(122)	166.6(5)	O(42)−Ti(3)−O(62)	81.1(4)
O(121)−Ti(2)−O(32)	96.9(5)	O(12)−Ti(3)−O(62)	82.3(4)
O(83)−Ti(2)−O(32)	167.4(5)	O(52)−Ti(4)−O(73)	99.8(4)
O(31)−Ti(2)−O(32)	84.1(4)	O(52)−Ti(4)−O(41)	90.6(4)
O(122)−Ti(2)−O(32)	82.5(4)	O(73)−Ti(4)−O(41)	95.6(4)
O(121)−Ti(2)−O(82)	164.6(4)	O(52)−Ti(4)−O(103)	100.2(4)
O(83)−Ti(2)−O(82)	84.9(5)	O(73)−Ti(4)−O(103)	89.3(4)
O(31)−Ti(2)−O(82)	96.8(4)	O(41)−Ti(4)−O(103)	167.2(4)
O(122)−Ti(2)−O(82)	80.0(4)	O(52)−Ti(4)−O(51)	86.0(4)
O(32)−Ti(2)−O(82)	82.6(4)	O(73)−Ti(4)−O(51)	170.4(5)
O(11)−Ti(3)−O(43)	94.8(5)	O(41)−Ti(4)−O(51)	91.9(4)
O(11)−Ti(3)−O(61)	95.0(5)	O(103)−Ti(4)−O(51)	82.2(4)
O(43)−Ti(3)−O(61)	101.0(5)	O(52)−Ti(4)−O(72)	172.6(4)
O(11)−Ti(3)−O(42)	98.2(5)	O(73)−Ti(4)−O(72)	85.2(4)
O(43)−Ti(3)−O(42)	85.5(4)	O(41)−Ti(4)−O(72)	83.4(4)
O(61)−Ti(3)−O(42)	164.8(5)	O(103)−Ti(4)−O(72)	85.2(4)
O(11)−Ti(3)−O(12)	83.1(4)	O(51)−Ti(4)−O(72)	89.8(4)
O(43)−Ti(3)−O(12)	164.5(4)	Ti(3)−O(12)−Bi(2)	141.5(4)
O(61)−Ti(3)−O(12)	94.5(4)	Ti(1)−O(22)−Bi(2)	144.5(4)

range between 1.730(9) and 2.141(10) Å with the Bi−O bond distances ranging between 2.175(10) and 2.808(16) Å. The bismuth atoms are found to be five- or six-coordinate (Figure 8). The metal oxygen bond lengths compare favorably to those in similar molecules.[25]

Table 5. Bond Lengths [Å] and Angles [deg] for $C_{70}H_{42}Bi_2O_{30}Ti_3$ (**4**)

Bi(1)−O(23)	2.238(4)	Ti(3)−O(13)	2.008(4)
Bi(1)−O(43)	2.309(4)	Ti(3)−O(72)	2.019(4)
Bi(1)−O(32)	2.321(4)	Ti(3)−O(82)	2.046(4)
Bi(1)−O(73)	2.417(4)	Ti(4)−O(51)	1.838(4)
Bi(1)−O(42)	2.476(4)	Ti(4)−O(61)	1.844(4)
Bi(1)−O(22)	2.607(4)	Ti(4)−O(41)	1.865(4)
Bi(1)−O(33)	2.623(4)	Ti(4)−O(52)	2.018(4)
Bi(2)−O(93)	2.200(4)	Ti(4)−O(62)	2.054(4)
Bi(2)−O(103)	2.209(4)	Ti(4)−O(42)	2.076(4)
Bi(2)−O(83)	2.344(4)	Ti(5)−O(11)	1.832(4)
Bi(2)−O(53)	2.444(4)	Ti(5)−O(101)	1.848(4)
Bi(2)−O(92)	2.496(4)	Ti(5)−O(21)	1.862(4)
Ti(3)−O(71)	1.816(4)	Ti(5)−O(12)	2.045(4)
Ti(3)−O(81)	1.845(4)	Ti(5)−O(22)	2.083(4)
Ti(3)−O(63)	1.985(4)	Ti(5)−O(102)	2.093(4)
O(23)−Bi(1)−O(43)	82.35(14)	O(23)−Bi(1)−O(42)	135.82(13)
O(23)−Bi(1)−O(32)	81.96(15)	O(43)−Bi(1)−O(42)	53.74(12)
O(43)−Bi(1)−O(32)	77.24(14)	O(32)−Bi(1)−O(42)	83.62(14)
O(23)−Bi(1)−O(73)	80.96(15)	O(73)−Bi(1)−O(42)	88.52(15)
O(43)−Bi(1)−O(73)	71.56(14)	O(23)−Bi(1)−O(22)	52.90(13)
O(32)−Bi(1)−O(73)	146.04(14)	O(43)−Bi(1)−O(22)	135.25(12)
O(32)−Bi(1)−O(22)	95.09(14)	O(81)−Ti(3)−O(13)	88.48(17)
O(73)−Bi(1)−O(22)	97.64(15)	O(63)−Ti(3)−O(13)	169.27(16)
O(42)−Bi(1)−O(22)	170.46(12)	O(71)−Ti(3)−O(72)	86.51(16)
O(23)−Bi(1)−O(33)	104.09(15)	O(81)−Ti(3)−O(72)	173.49(17)
O(43)−Bi(1)−O(33)	126.39(13)	O(63)−Ti(3)−O(72)	90.25(16)
O(32)−Bi(1)−O(33)	52.14(14)	O(13)−Ti(3)−O(72)	87.16(16)
O(73)−Bi(1)−O(33)	161.55(14)	O(71)−Ti(3)−O(82)	175.30(16)
O(42)−Bi(1)−O(33)	99.25(13)	O(81)−Ti(3)−O(82)	85.97(16)
O(22)−Bi(1)−O(33)	72.77(13)	O(63)−Ti(3)−O(82)	84.83(16)
O(93)−Bi(2)−O(103)	79.49(15)	O(13)−Ti(3)−O(82)	84.70(16)
O(93)−Bi(2)−O(83)	77.82(14)	O(72)−Ti(3)−O(82)	88.82(15)
O(103)−Bi(2)−O(83)	82.18(14)	O(51)−Ti(4)−O(61)	99.60(17)
O(93)−Bi(2)−O(53)	74.82(15)	O(51)−Ti(4)−O(41)	94.84(18)
O(103)−Bi(2)−O(53)	89.00(15)	O(61)−Ti(4)−O(41)	97.14(18)
O(83)−Bi(2)−O(53)	152.36(14)	O(51)−Ti(4)−O(52)	84.34(17)
O(93)−Bi(2)−O(92)	55.20(15)	O(61)−Ti(4)−O(52)	99.96(18)
O(103)−Bi(2)−O(92)	134.14(14)	O(41)−Ti(4)−O(52)	162.78(16)
O(83)−Bi(2)−O(92)	81.79(15)	O(51)−Ti(4)−O(62)	165.00(18)
O(53)−Bi(2)−O(92)	85.85(15)	O(61)−Ti(4)−O(62)	84.32(16)
O(71)−Ti(3)−O(81)	98.72(17)	O(41)−Ti(4)−O(62)	99.05(17)
O(71)−Ti(3)−O(63)	94.62(18)	O(52)−Ti(4)−O(62)	80.71(16)
O(81)−Ti(3)−O(63)	93.16(17)	O(51)−Ti(4)−O(42)	95.31(17)
O(71)−Ti(3)−O(13)	95.61(18)	O(61)−Ti(4)−O(42)	165.08(16)
O(41)−Ti(4)−O(42)	81.73(16)	O(101)−Ti(5)−O(22)	99.37(17)
O(52)−Ti(4)−O(42)	81.22(15)	O(21)−Ti(5)−O(22)	82.15(16)
O(62)−Ti(4)−O(42)	81.19(15)	O(12)−Ti(5)−O(22)	79.67(15)
O(11)−Ti(5)−O(101)	98.01(19)	O(11)−Ti(5)−O(102)	98.99(17)
O(11)−Ti(5)−O(21)	95.37(18)	O(101)−Ti(5)−O(102)	83.00(16)
O(101)−Ti(5)−O(21)	94.89(18)	O(21)−Ti(5)−O(102)	165.64(17)
O(11)−Ti(5)−O(12)	83.90(17)	O(12)−Ti(5)−O(102)	81.05(15)
O(101)−Ti(5)−O(12)	164.04(17)	O(22)−Ti(5)−O(102)	84.18(15)
O(21)−Ti(5)−O(12)	100.73(17)	Ti(5)−O(22)−Bi(1)	139.49(17)
O(11)−Ti(5)−O(22)	162.59(18)	Ti(4)−O(42)−Bi(1)	135.64(18)

Solid samples of **3** were found to contain solvent located both in the lattice and in the interior of the molecule itself. Interestingly, a single molecule of water was found to occupy the center of the molecule of **3**. In the crystal lattice, the water molecule is four-coordinate and exhibits a distorted tetrahedral geometry. The water molecule is presumably weakly bound to the bismuth atoms ($d_{Bi(1)-O(1)} = 2.783(9)$ Å, $d_{Bi(2)-O(1)} = 3.004(9)$ Å) through lone pair electrons and also interacts with two salicylate ligand oxygen atoms (O(32) and O(102)) through hydrogen bond interactions ($d_{O(32)-O(1)} = 2.757(14)$ Å, $d_{O(102)-O(1)} = 2.83$ Å). A third possible, but weaker, interaction was also detected between the water molecule and O(72) ($d_{O(72)-O(1)} = 2.92$ Å). These bond distances are comparable with distances that have been reported for other hydrates, which have been reported to range from 2.6 to 2.9 Å in length.[26]

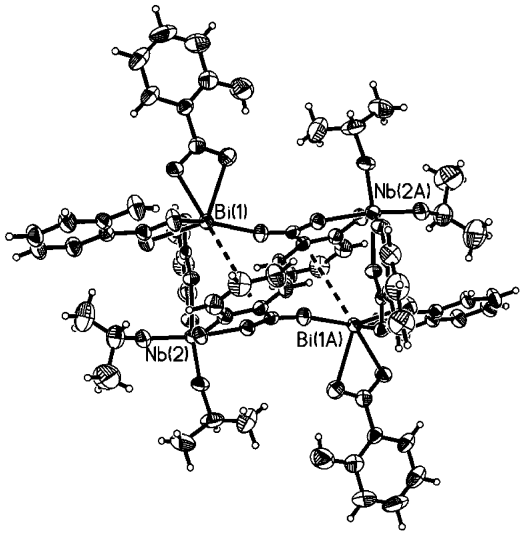

Figure 1. ORTEP representation of **1a**. Thermal ellipsoids are drawn at the 50% probability level. The π-interactions between bismuth and the salicylate ring are represented by broken lines.

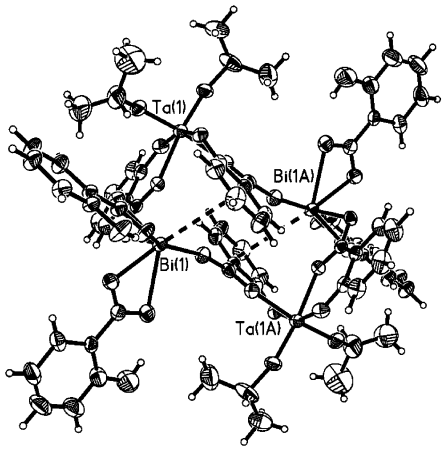

Figure 2. ORTEP representation of **2a**. Thermal ellipsoids are drawn at the 50% probability level. The π-interactions between bismuth and the salicylate ring are represented by broken lines.

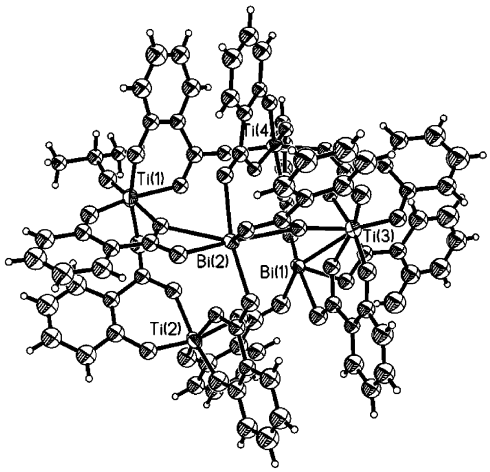

Figure 3. ORTEP representation of **3**. Thermal ellipsoids have been drawn at the 30% probability level for clarity.

(25) Asato, E.; Katsura, K.; Arakaki, T.; Mikuriya, M.; Kotera, T. *Chem. Lett.* **1994**, 2123−2126.

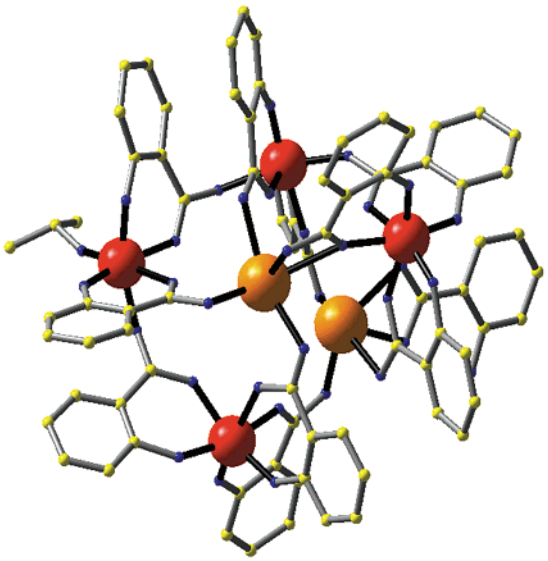

Figure 4. Winray representation of **3**.[42] Metal atoms have been emphasized to illustrate the connectivity of the complex. Hydrogen atoms have been omitted for clarity. Color scheme: orange, bismuth; red, titanium; blue, oxygen; yellow, carbon.

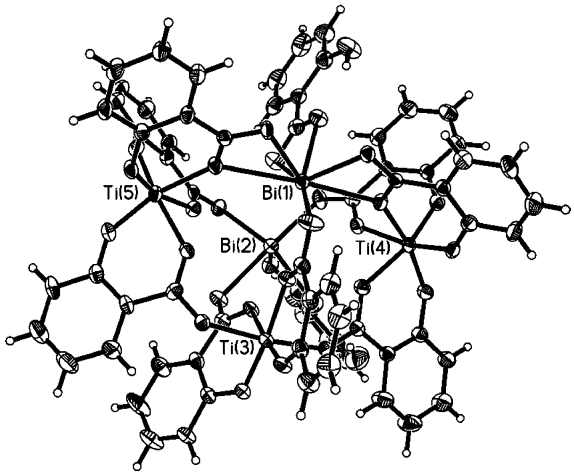

Figure 5. ORTEP representation of **4**. Thermal ellipsoids are drawn at the 30% probability level for clarity.

The assignment of the oxygen atom as water was based on the long bond distances of the atom to the metal center and charge balance requirements of the entire complex. Hydrated bismuth atoms have recently been characterized as trifluoromethanesulfonate salts.[27,28] In these samples, the Bi−O_{water} bond lengths lie in the range 2.448−2.577 Å. This is considerably longer than the reported bond distances for μ_2 bridging oxo ligands, which lie in the range 2.023−2.123 Å.[29] The long Bi−O_{water} bond in **3** can be rationalized as rising from bridging orientation of the water molecule. This orientation would be expected to give rise to longer bond distances, compared to the terminal orientation found in the hydrated bismuth triflate structure. The charge balance requirements of the metal centers in the complex are also fully satisfied by the salicylate and alkoxide ligands alone. This further suggests that the identity of the oxygen atom in the structure is water, which would allow the complex to remain neutral. Spectroscopic characterization of the water by ^{1}H NMR and FTIR was inconclusive because of the presence of residual hydroxyl groups in the salicylate ligands.

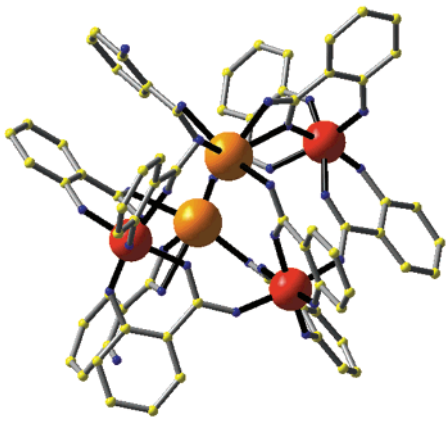

Figure 6. Winray representation of **4**.[42] Metal atoms have been emphasized to illustrate the connectivity of the complex. Hydrogen atoms have been omitted for clarity. Color scheme: orange, bismuth; red, titanium; blue, oxygen; yellow, carbon.

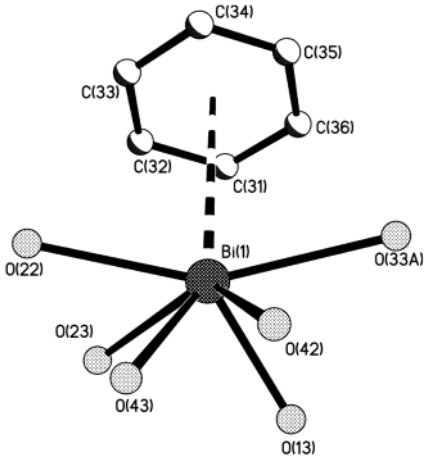

Figure 7. Representation of the coordination environment of the bismuth atoms in **1a** and **2a**.

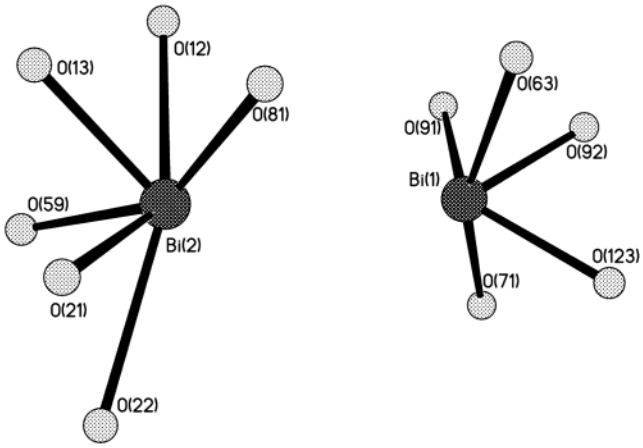

Figure 8. Representation of the bismuth coordination environment in **3**.

(26) Wells, A. F. *Structural Inorganic Chemistry*, 5th ed.; Oxford Press: Oxford, 1984.
(27) Frank, W.; Reiss, G. J.; Schneider, J. *Angew. Chem., Int. Ed. Engl.* **1995**, *34*, 2416−2417.
(28) Näslund, J.; Persson, I.; Sandström, M. *Inorg. Chem.* **2000**, *39*, 4012−4021.
(29) Hassan, A.; Breeze, S.; Courtenay, S.; Deslippe, C.; Wang, S. *Organometallics* **1996**, *15*, 5613−5621.

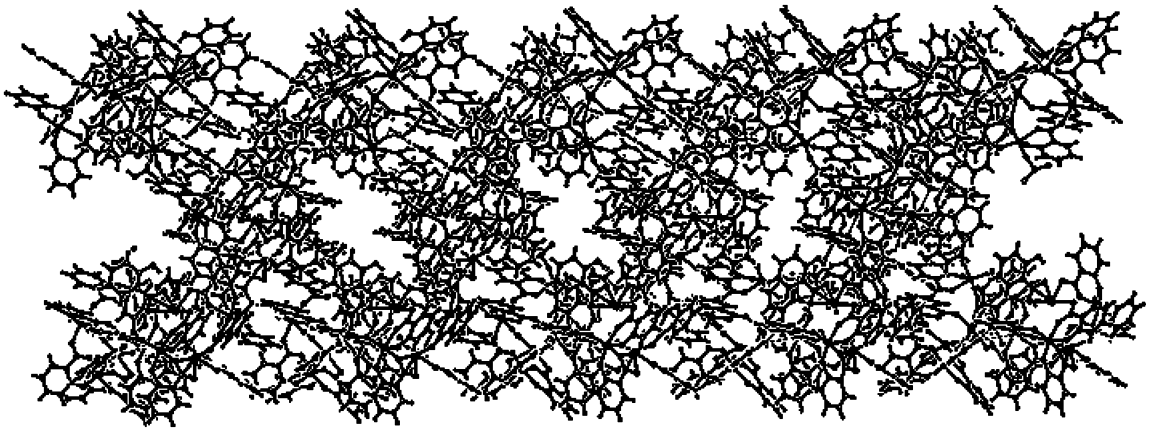

Figure 9. Ball-and-stick packing diagram of **3** detailing the void area found in the crystal lattice.

Modeling of the crystallographic data of **3** using the program PLATON reveals that the solid-state structure contains void area equal to 2020 Å^3, or 22% of the unit cell (Figure 9). Disordered solvent molecules that would contribute to a fairly high residual electron density that is observed in the structure presumably occupy this void area. Assuming that a single molecule of 2-propanol has a volume of approximately 110 Å^3, then it appears that as many as 20 molecules of solvent may be located in the unit cell. Although many of the included molecules are lost during the isolation of the material, it was possible to confirm the presence and identity of the lattice solvent through a variety of techniques. The elemental analysis of **3** agreed with the inclusion of approximately three molecules of 2-propanol in the crystal lattice. Further,because the molecules assayed consistently high for carbon and hydrogen, it was concluded that the lattice solvent was not exclusively water. The results of elemental analysis were confirmed through careful interrogation of the samples by proton NMR. Fresh samples of **3** demonstrate two distinct methyne resonances at $\delta = 3.98$ and 4.76 ppm. The two methyne peaks integrate to approximately 3.3:1 and can be correlated to the free lattice solvent and the single 2-propyl group that is located on **3**, respectively. The assignment of the peaks is supported by examining the NMR spectra of samples of **3** that have either been aged for several months or dried under vacuum (10^{-7} Torr) for several days. In these cases, the resonance at 4.76 ppm is unchanged while that at 3.98 is reduced or absent. This low field shift of the methyne proton in the 2-propoxide ligands coordinated to titanium relative to the free alcohol has been observed for other complexes as well.[30] The NMR analysis is supported by TGA analysis, which demonstrates a quick loss of volatile material comprising approximately 9.7% of the mass of the sample (calculated for three molecules of 2-propanol: 9%). It is difficult to conclude from these experiments if the coordinated water is also lost from the lattice, as the calculated change in mass for loss of the single water molecule is very small.

(30) Motoyama, Y.; Tanaka, M.; Mikami, K. *Inorg. Chim. Acta* **1997**, *256*, 161−163.

The mass spectrum of **3** displays the parent ion at the expected location. Isotopic matching of the observed spectrum supports the assignment of the parent ion peak. In addition to the parent ion, the spectrum of **3** demonstrates 12 fragments corresponding to the successive loss of salicylate ions or 2-propoxide ions from the parent complex. Three peaks heavier than the parent ion were also observed in the spectrum. These can be assigned to products resulting from exchange reactions or rearrangements of the parent ion.

Compound **4** was synthesized by allowing Ti{OCH-$(CH_3)_2$}$_4$ to react with the product of the reaction of triphenyl bismuth and 4 equiv of salicylic acid in toluene at room temperature. These are similar reaction conditions to what was employed for the syntheses of **1b** and **2b**. Careful recrystallization of the product mixture led to the growth of deep orange prisms of **4** along with the deposition of a yellow powder. The crystals were isolated and characterized both crystallographically and spectroscopically.

The overall structure of **4** was found to resemble that of **3**, but it contained one less titanium atom, one less salicylate ion, and no residual alkoxide ligands. The Ti−O bond lengths in **4** range from 1.816(4) to 2.093(4) Å. This agrees well with what is observed in **3**. The geometry of the transition metal centers, including bond lengths and angles, is similar to what has been observed in the structure of **3**. Compound **4** exhibits Bi−O bond distances that range between 2.200(4) and 2.623(4) Å. Like **3**, the two bismuth centers in the compound exhibit different coordination numbers (Figure 10). In this case, one of the bismuth atoms is five-coordinate, and the other, seven-coordinate. Under the conditions that were used in the synthesis and purification of **4**, the molecule cocrystallizes with three solvent molecules of dichloromethane. The solvent molecules were ordered in the crystal lattice and refined well.

The thermal decompositions of **1a**−**4** were investigated by TGA. Compound **1a** begins to decompose at 200 °C with a mass loss of 22%. This is followed by two additional mass losses of 27% and 16% at approximately 280 °C and 385 °C, respectively. Compound **2a** is very similar with its decomposition beginning at 210 °C with a mass loss of 14%. This is followed by two additional mass losses of 26% and

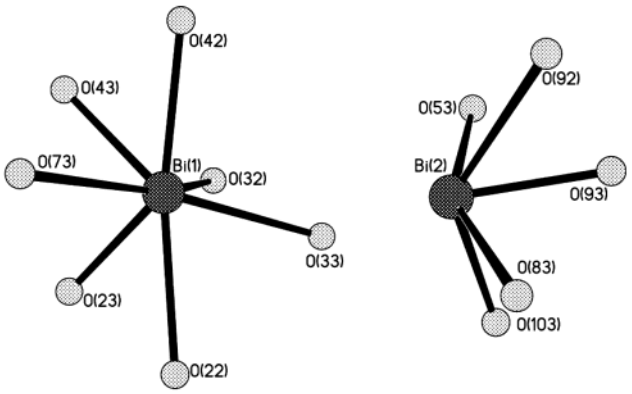

Figure 10. Representation of the bismuth coordination environment in **4**.

12% at 305 °C and 397 °C, respectively. Mass losses of 62% and 57% are required for the conversion of **1a** and **2a** to metal oxide, respectively. This agrees with the total observed losses (62% and 55%, respectively). The thermograms of compounds **1b** and **2b** are similar to those of **1a** and **2a**, asexpected. The decomposition of **1b** and **2b** occurs at slightly lower temperature than that of **1a** and **2a.** Compound **1b** demonstrates three successive mass losses at 110, 278, and 401 °C, totaling 59% of the total sample weight. This corresponds well with the calculated value of 61% mass loss for the conversion of **1b** to $BiNbO_4$. Similarly, **2b** demonstrates three distinct mass losses at 124, 302, and 365 °C totaling 56% of the sample, which agrees exactly with the calculated mass loss required to convert the sample to metal oxide (56%).

As mentioned earlier, the thermogram of **3** shows a quick mass loss of 9.7% starting at approximately 35 °C, probably correlating to the loss of solvent from the crystal lattice. This has been confirmed experimentally by drying a sample of the cluster under dynamic vacuum for 1 week. In this case, the sample lost approximately 12% of its original mass, which, within the limits of experimental error, agrees well with the observations of single-crystal X-ray analysis and ^{1}H NMR. Decomposition of **3** begins at approximately 270 °C with a mass loss of 42%. This is followed by a second mass loss at 390 °C of 19%. A phase change in the material is observed at 427 °C. The final oxide is obtained at 500 °C. Conversion of **3** completely to metal oxides requires the 60% mass loss from the sample. The final two steps of the thermal decomposition of **3** represent a 61% mass loss, which agrees with the expected value.

The thermal decomposition of **4** is similar to **3**. The molecule decomposes in two steps. Loss of lattice solvent from the sample occurs between 37 °C and 152 °C, represents a loss of 12% of the sample, and is consistent with approximately three molecules of dichloromethane per molecule of complex (ca. 12%). This is in agreement with the results of the X-ray experiments and elemental analysis. Decomposition of the complex occurs in a single step beginning at 278 °C and reflects a 64% loss of mass from the sample. This total mass loss observed for the sample is in good agreement with the calculated mass loss required toconvert **4**·$3CH_2Cl_2$ to the metal oxide (calcd 75%, obsd 76%). The final oxide is obtained at 410 °C.

The nature of the oxide that is obtained from each of the complexes was probed by powder X-ray diffraction. Samples of heterobimetallic complexes were converted to the crystalline materials by calcining at temperatures in excess of 700 °C for 3 h in air. The product was slowly cooled to room temperature to produce a white or pale yellow crystalline solid in all cases. The product was ground to produce a finely dispersed powder that was used in the analysis. It was observed that calcining the samples at lower temperatures than those used in these experiments produced only amorphous material. The identity of the product materials as the heterobimetallic oxides was confirmed by comparing the powder diffraction patterns to accepted standards, using the computer program JADE.[31] It has been demonstrated that **1a** and **2a** decompose with heating at 700 °C to produce the orthorhombic phase (the low temperature form) of $BiMO_4$ (M = Nb, Ta), as the major crystalline phase. Samples of **1a** were also found to contain the bismuth-rich heterobimetallic oxide $Bi_5Nb_3O_{15}$. The oxide of **2a** was found to contain Bi_2O_3. No crystalline bismuth-rich heterobimetallic oxide was detected in the sample. Complex **3** decomposed to form the bismuth-rich oxide $Bi_4Ti_3O_{12}$ as the major crystalline phase. The expected product $Bi_2Ti_4O_{11}$ was only detected in ca. 30% relative abundance to the bismuth-rich phase. Complex **4** was found to react similarly on heating to produce $Bi_4Ti_3O_{12}$ and $Bi_2Ti_4O_{11}$ in a ca. 90:10 ratio.

Solution phase measurements of the molar masses of complexes **1b** and **3** in THF solution gave results of 1227 and 1960 g·mol^{-1}, respectively. Calculated masses for the complexes in the solid state are 1876.61 and 2152.63 g·mol^{-1}, respectively. These results are consistent with the conjecture that **3** dissolves unchanged but that **1b** dissociates into a solvated monomer (cf. the molar mass of monomer·2THF is 1190 g·mol^{-1}). While there is some uncertainty associated with the molar mass determined in this manner, when these data are coupled with the ^{1}H NMR results, it creates a convincing case that molecules **1a** and **1b** dissociate in solution (Figure 11).

Discussion

The use of bifunctional ligands such as salicylic acid offers a direct "one-pot" synthesis for heterobimetallic complexes containing bismuth. The fact that the solubility of the bismuth−salicylate complex changes as the amount of salicylic acid in the reaction mixture is altered implies that there is an interaction of the excess salicylic acid with the complex. It seems likely that the complex that is formed from an exact 1:3 ratio of bismuth to salicylic acid is oligomeric or polymeric, existing as $[Bi(salH)_3]_n$ (salicylateH = O_2-CC_6H_4-2-OH). Coordination polymerization is common for

(31) *JADE, XRD Pattern-Processing for the PC* 2.1; Materials Data, Inc.: Livermore, CA, 1994.

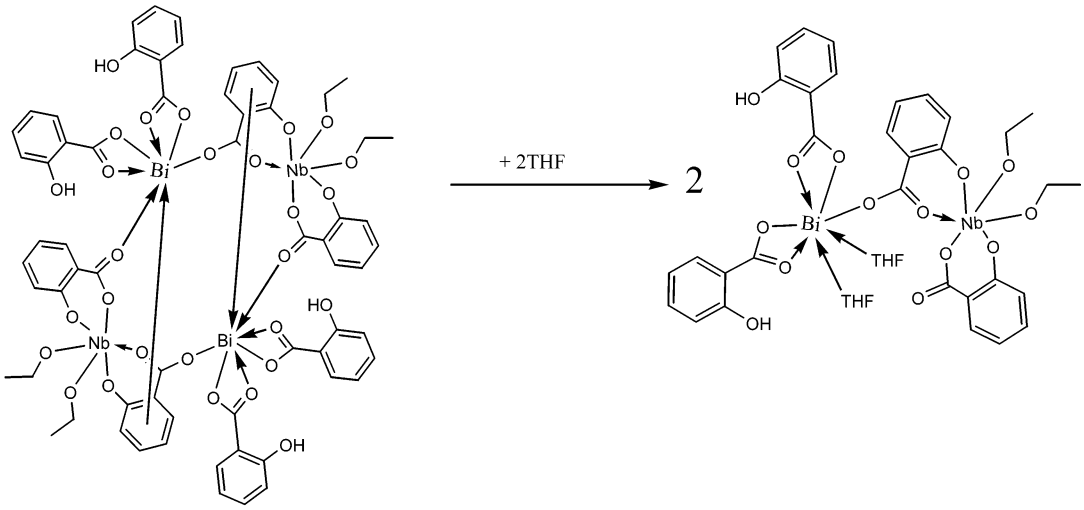

Figure 11. Dissociation of **1a** into a solvated monomer.

Lewis acidic bismuth centers, which are often observed with high coordination numbers, and elemental analysis of the complex supports this formulation.[14,32]

Bismuth (III) centers with electronegative ligands are strongly Lewis acidic, so it is reasonable to conclude that the metal is able to coordinate oxygen atoms of adjacent complexes resulting in the oligomerization or polymerization. It appears that excess salicylic acid disrupts these additional interactions, probably through the formation of salicylate adducts such as $Bi(salH)_3(salH_2)$. This explains the higher solubility of the product in the presence of excess salicylic acid. Investigations into the nature of these complexes, which are difficult to isolate free from excess salicyclic acid, are ongoing.

Drawings **I**−**VI** illustrate possible coordination modes of the salicylate ligand with bismuth or with bismuth and a transition metal. Of these, the terminal mode **IV** has not been observed in this class of complexes. The structural observations for **1a**, **2a**, **3**, and **4** suggest that bismuth prefers to bond through the carboxylate functionality of the salicylate ligand (**I**, **V**, **VI**), while transition metals associate with both the hydoxyl and carboxylate functional groups to form a six-membered chelate ring (**II**). However, this does not rule out the possibility of chelating salicylate ligands that are associated with bismuth through both functional groups, particularly in absence of other metal species. The fact that $[Bi(O_2CC_6H_4OH)_3]_n$ is yellow may indicate that the hydroxyl groups of the salicylate ligands are interacting with the metal center (**III**). This theory is supported by IR studies of the complex, which demonstrate a ν(OH) peak at 3231 cm^{-1}. This is at a higher frequency than the free acid (ν-(OH) = 3059 cm^{-1}), suggesting that there is interaction between the phenolic oxygen and the bismuth atom. This conjecture is also supported by the fact that reactions carried out using triphenyl bismuth and benzoic or methacrylic acid produce only a white product. Furthermore, many known phenoxycomplexes of bismuth such as $Bi(OC_6H_3\text{-}2,6\text{-}(CH_3)_2)_3$ and $[Bi(OC_6F_5)_3(\mu_6\text{-}C_7H_8)]_2$ are yellow.[13,33,34]

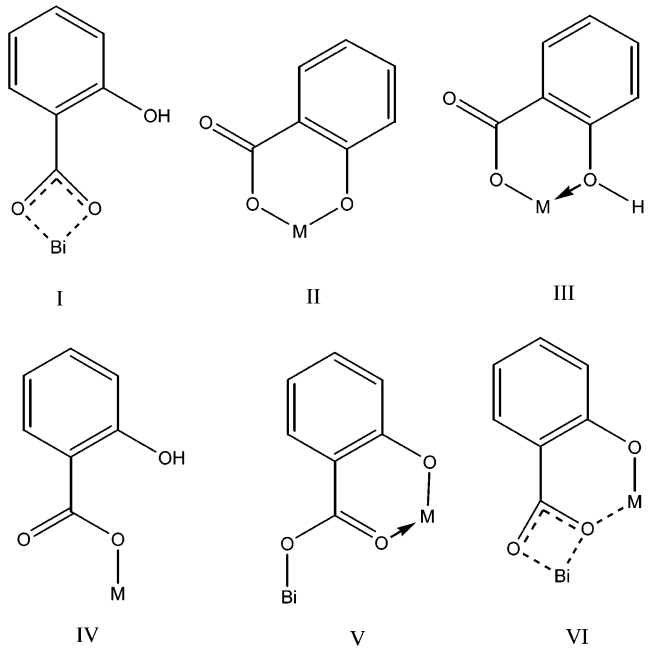

Given the high oxophilicity of the group IV and V transition metals, one of the most interesting outcomes of the syntheses is the noticeable lack of oxo ligands and the relative stability of residual alkoxide moieties in **1**−**4**. This is particularly surprising for complexes **1**−**3** because of the fact that the syntheses of these compounds were performed in the presence of excess carboxylic acid. Under these conditions, it is known that the unreacted acid can undergo esterification with liberated alcohol or with the solvent yielding water as a byproduct and leading to the formation of oxo or hydroxo ligands. However, these complexes appear to exhibit exceptional stability toward hydrolysis. Compound **3** was observed to cocrystallize with water with no apparent

(32) Asato, E.; Katsura, K.; Mikuriya, M.; Fuji, T.; Reediijk, J. *Inorg. Chem.* **1993**, *32*, 5322−29.

(33) Jones, C. M.; Burkhart, M. D.; Bachman, R. E.; Serra, D. L.; Hwu, S.-J.; Whitmire, K. H. *Inorg. Chem.* **1993**, *32*, 5136.

(34) Evans, W. J.; Hain, J. H.; Ziller, J. W. *Chem. Commun.* **1989**, 1628.

hydrolysis or decomposition. Attempts to modify **3** by addition of $^1/_2-1$ mmol of water/mmol of titanium during various stages of the synthesis still gave **3** as the only isolable product.

The π-interaction of the aromatic ring of the salicylate ligand with the bismuth center in **1a** and **2a** (Figure 7) suggests that the bismuth atom in these complexes is relatively electron deficient. This type of interaction has been documented in other complexes that contain bismuth coordinated to electronegative ligands, such as petafluorophenoxide,[13,33,35] trifluoroacetate,[36] and chloride.[37−39] The distances between the metal and the aromatic ring compare well with other compounds that have been reported by our group, namely $Bi_4(\mu_4\text{-}O)(\mu_2\text{-}OC_6F_5)_6\{\mu_3\text{-}OBi(\mu\text{-}OC_6F_5)_3\}_2(\mu_6\text{-}C_6H_5CH_3)$ and $[Bi(\mu\text{-}OC_6F_5)(OC_6F_5)_2(\mu_6\text{-}C_6H_5CH_3)]_2$ which have bismuth−ring centroid distances of 3.074(2) and 2.968(2) Å, respectively.[16] The bismuth−aromatic ring centroid distances in these molecules are shorter than in **1a** or **2a**, suggesting that the metal center in **1a** and **2a** is less electropositive than it is in the pentafluorophenoxy complexes, as might be expected.

Molar mass studies undertaken in coordinating solvents indicate that **3** dissolves unchanged, while **1b** demonstrates a significantly different molar mass in solution than in the solid state. These calculations can be correlated with the observed solid-state structures of the complexes. Compound **3** is assembled so that all of the metal centers in the complex are associated through a series of covalent bonds. These bonds provide the stabilization needed to protect the integrity of the complex when the molecule is dissolved. In contrast, **1b** is observed to be a dimer in the solid state, in which the two subunits of the complex are associated through dative interactions. These bonding modes are much weaker than what is observed in **3**, and solvation results in disruption of the dimeric structure. The monomers, in this case, appear to be stabilized though coordination interactions of several solvent molecules with the metal centers and are thought to exist in dynamic equilibrium with the dimeric complex.

Nuclear magnetic resonance studies of **1a**−**4** were not informative either because of the low symmetry of the complex and resultant large number of peaks (**3**, **4**) or the fact that apparent rapid ligand exchange of the salicylate ions produced very broad peaks in the aromatic region (**1a**, **2a**, **1b**, **2b**). In all cases, the alkoxide ligand resonances were clearly resolved. The protons adjacent to the alkoxide oxygen frequently demonstrated a significant downfield shift upon coordination, which is consistent with metal coordination.[30]

It is significant that the ^{1}H NMR spectra of **1a**, **2a**, **1b**, and **2b** demonstrate a single salicylate environment, whereas the spectra of **3** and **4** show the presence of numerous magnetically inequivalent salicylate ions. This strongly suggests that **1a**, **2a**, **1b**, and **2b** are able to undergo ligand exchange processes at a rate that is fast on the NMR time scale. Attempts to slow the rate of exchange to the point that individual salicylate environments could be resolved through cooling of the sample were not successful.

The IR spectra of complexes **1a**−**4** are complex and difficult to interpret. All of the complexes demonstrate a strong peak in the region of 3200−3600 cm^{-1}, which correlates to the O−H stretch of the singly deprotonated salicylate ligands in the structure. The coordinated water molecule observed in the solid-state structure of **3** should also produce a distinct peak in this region. However, this peak overlaps with the stronger phenolic O−H stretch and was consequently unobservable. The antisymmetric carbonyl stretch of free carboxylic acids is known to occur in the range 1800−1550 cm^{-1}, while the symmetric carbonyl stretch is known to lie in the range approximately 1450−1370 cm^{-1}.[40] For free salicylic acid, the ν_{as}(COO) and ν_s(COO) are observed to be 1662 and 1441 cm^{-1}, respectively. The interactions of the ligand with the metal centers in complexes discussed in this paper were probed through monitoring the shift in frequency of the ν_{as}(COO) and ν_s(COO) peaks of the free acid. For all of the complexes, the ν_{as}(COO) peaks were found to be significantly shifted toward 1550 cm^{-1}. This has been noted to be indicative of ionization of the carboxyl group and supports the results of the single crystal X-ray studies in indicating that no protons are associated with the carboxylic functional group of the ligands. The symmetric carbonyl stretch was found to have shifted to approximately 1350 cm^{-1} for the complexes. This peak has been used to provide structural information regarding the mode of ligand association between one or more metal centers in simple cases.[41] In our complexes, it is difficult or impossible to make accurate assignments of specific bonding modes because of the complexity of the structures and resultant spectra; however, the range of the frequencies of the peaks that are observed for these complexes is suggestive of either bidentate (**I**) or bidentate/bridging coordination (**V** and **VI**) by the carboxylate ligand. This observation, like that for the antisymmetric carbonyl peak, agrees with the findings of the single-crystal structure analyses.

All of the compounds were easily converted to metal oxides when the samples were heated in air. TGA analysis indicates that the complexes undergo complete thermal decomposition on heating to 600 °C. Thermal decomposition studies carried out under nitrogen gave similar results. This suggests that all of the oxygen atoms necessary for the production of the oxide may be obtained from the initial complex. The bimetallic oxides obtained at these temperatures are amorphous. Heating the molecular samples to greater than 700 °C produces crystalline samples of the bimetallic oxides. Under the conditions that were explored

(35) Jones, C. M.; Burkhart, M. D.; Whitmire, K. H. *Angew. Chem., Int. Ed. Engl.* **1992**, *31*, 451.
(36) Frank, W.; Reiland, V.; Reiss, G. J. *Angew. Chem., Int. Ed.* **1998**, *37*, 2984−2985.
(37) Frank, W.; Schneider, J.; Muller-Becker, S. *Chem. Commun.* **1993**, 799−800.
(38) Frank, W.; Muller-Becker, S.; Schneider, J. *Z. Anorg. Allg. Chem.* **1993**, *619*, 1073−1082.
(39) Frank, W.; Reiland, V. *Acta Crystallogr., Sect. C* **1998**, *54*, 1626−1628.
(40) *Lange's Handbook of Chemistry*, 15th ed.; McGraw-Hill: New York, 1999.
(41) Deacon, G. B.; Phillips, R. J. *Coord. Chem. Rev.* **1980**, *33*, 227−250.
(42) Soltek, R. *Winray GL*; Zurük zum Anorganisch-Chemischen Institut: Heidelberg, 2000.

in these studies, mixtures of oxides were obtained for all of the samples. The higher temperatures required to produce crystalline samples may favor disproportionation and redistribution of metal atoms in the oxide system and allow the formation of the stable bismuth-rich perovskite phase in the case of **3** and **4**. In all cases, the conditions required to produce the bimetallic oxide are substantially milder than those required under conventional solid-state synthesis conditions. For example, the formation of a low temperature form of $BiTaO_4$ with an orthorhombic unit cell ($a = 4.957$ Å, $b = 11.763$ Å, $c = 5.633$ Å) has been reported to occur previously at 900 °C for 18 h.[27] We have obtained the same material from the conversion of **2a** to the oxide through heating at 700 °C for 3 h.

Conclusion

Bifunctional hydroxy−carboxylate ligands offer a convenient and direct route to the synthesis of heterobimetallic complexes. We have demonstrated that it is possible to effect the construction of these compounds in a rational and stepwise manner by choosing ligands whose functional group protons have differing acidities. The compounds synthesized in this manner demonstrate both good solubility in a variety of organic solvents and excellent stability against unwanted hydrolysis. The materials can be converted to bimetallic oxides by heating in an oxygen-containing atmosphere at 600 °C. Powder X-ray diffraction and TGA studies of the oxides indicate that the ratio of metals in the molecular precursor influences the ratio of metals in the final oxide. The titanium containing complexes gave the bismuth-rich $Bi_4Ti_3O_{12}$ phase along with the $Bi_2Ti_4O_{11}$ phase expected on the basis of the metal stoichiometry of the precursor.

Acknowledgment. We would like to thank the Robert A. Welch foundation and the NSF for support of this work. J.H.T. would like to thank Dr. Terry Marriott for aid in collecting the mass spectra of complex **3** and Dr. Larry Alemany for aid in low temperature NMR experiments and for helpful discussion.

Supporting Information Available: Full presentation of the crystallographic data and experimental parameters including atomic coordinates, bond lengths and angles, anisotropic displacement parameters, and hydrogen atom coordinates (CIF). Detailed numbering schemes for the structures of **1a**, **2a**, **3**, and **4**, representative powder X-ray diffraction patterns, TGA spectra, and IR data. This material is available free of charge via the Internet at http://pubs.acs.org.

IC0255454